RSC Advances

PAPER

View Article Online
View Journal | View Issue



Cite this: *RSC Adv.*, 2019, **9**, 34827

# $SF_6$ abatement in a packed bed plasma reactor: study towards the effect of $O_2$ concentration†

Yuan Tian,[a] Xiaoxing Zhang,[a] Bowen Tang,*[a] Zhaolun Cui,*[a] Guozhi Zhang,[a] Zhenwei Chen[a] and Hao Wang[b]

$SF_6$ is a greenhouse gas with extremely high global warming potential value (GWP). In this paper, oxygen and a packed bed plasma reactor (PBR) were applied to remove it. The synergistic effect between oxygen and PBRs was evaluated by the destruction and removal efficiency (DRE) and energy yield (EY) at different oxygen concentrations. The results show that excessive oxygen weakened the micro-discharge in a PBR to suppress $SF_6$ degradation while the addition of a proper amount of oxygen (1–4%) can improve the DRE and EY. 2% $O_2$ in the system had the best promoting effect on the destruction of 6–10% $SF_6$, which made the maximum energy yield (EY) increase by 50.99% to 37.99 g $kW^{-1}$ $h^{-1}$ ($SF_6$ concentration was 10%, flow rate was 150 mL $min^{-1}$). Moreover, in the flow rate range of 100 mL $min^{-1}$ to 250 mL $min^{-1}$, the DRE decreased and the EY increased with the flow rate. In addition, the selectivity of different products were affected by the oxygen concentration. For 6% $SF_6$, $SO_2F_2$ selectivity was always the highest while $SO_2$ was always the lowest; when the oxygen concentration did not exceed 2%, $SOF_2$ selectivity was higher than $SOF_4$, otherwise, $SOF_4$ selectivity was higher than $SOF_2$. This paper provided experimental support for better understanding of the effect of additional gas concentration on $SF_6$ decomposition in a PBR.

Received 21st July 2019
Accepted 10th October 2019

DOI: 10.1039/c9ra05629g

rsc.li/rsc-advances



## 1 Introduction

$SF_6$ is widely used in the power industry as an excellent insulating gas, but due to its extremely high global warming potential value (GWP), it is also listed as one of the six restricted gases by the Kyoto Protocol.[1] However, it is still used in large quantities because there is no reliable $SF_6$ replacement gas.[2–4] It is estimated that the current global $SF_6$ usage is above 10 000 tons, and more than 80% is used in the power industry.[5] Every year, the power industry is facing the problem of recycling and emission of huge amounts of $SF_6$. Therefore, how to deal with $SF_6$ has become a hot issue in the field of environmental protection.

Scholars have done a lot of research on the treatment of low concentrations $SF_6$. Methods like radio frequency plasma, microwave plasma and photolysis degradation were applied to remove it,[6–8] but the effective treatment concentrations of the above studies were no more than 1%. However, the concentration of $SF_6$ used in power industry is high. Up to now, scholars around the world are still lacking in research on high concentration $SF_6$ treatment.

Dielectric barrier discharge (DBD) technology has been widely used in the reduction of industrial exhaust due to its high efficiency and economy.[9,10] DBD can generate reactive species in the discharge gap to physically and chemically interact with the waste gas molecules resulting in the decomposition of them.[11] In recent years, Zhang *et al.* used DBD plasma to destruct $SF_6$ (2%) under static conditions. Although high destruction and removal efficiency (DRE) was obtained, there were still some problems such as low energy yield (EY) and long treatment cycle.[11,12] Those obstacles inhibit the further application of DBD.

Changing gas composition has been applied to enhance the processing efficiency of DBD reactors. Lee *et al.* destructed $SF_6$ in $Ar/N_2/O_2$ system to study the effects of additional gases on DBD reduction of $SF_6$.[13] Zhang *et al.* added $NH_3$ to the DBD reactor to promote the $SF_6$ destruction.[14] The above studies show that the additional gases can significantly impact the EY of DBD treatment of $SF_6$. Meanwhile, some research has shown that packing materials in DBD reactors can greatly improve the EY of DBD.[15–18] Lee *et al.* used packed bed reactors (PBRs, DBD reactors containing packing materials) to degrade $SF_6$ and $CF_4$.[18] Both methods have a greatly influence on the EY of $SF_6$ abatement, but there is no report on the synergistic effect of oxygen on PBRs degradation of high concentration $SF_6$. If oxygen and packing materials can obtain good synergy, it will provide the possibility for PBRs to handle flowing high concentration $SF_6$ (2–10%). The treatment of flowing high concentration $SF_6$ not only can

[a]School of Electrical Engineering and Automation, Wuhan University, Wuhan 430072, China. E-mail: Zhaoluncui@163.com; sm0719@yeah.net

[b]State Grid Hubei Electric Power Company Maintenance Company, Wuhan 430050, China

† Electronic supplementary information (ESI) available. See DOI: 10.1039/c9ra05629g

improve the processing efficiency but also can save a large amount of carrier gas, which has significant economic benefits. In addition, the effect of oxygen concentration on the products selectivity has not been studied, although the relationship between them is crucial for the waste gas treatment.

Oxygen is a commonly used oxidant. Its active O radicals in the plasma region can oxidize low fluorine sulfides, thereby promoting the degradation of $SF_6$, but it is also an electronegative gas, excessive oxygen in the system also has an adverse effect on destruction.[13,19,20] Therefore, there is a balance to be achieved between the reaction of O radicals with low fluorine sulfides, and the negative effect of oxygen on $SF_6$ degradation in PBRs. This paper aims to study the synergistic effect of different concentration of oxygen and PBRs, and to investigate the selective effect of oxygen concentration on $SF_6$ degradation by-products, so as to provide guidance for further treatment of $SF_6$.

# 2 Method

## 2.1. Test platform

The overall schematic and physical picture of the PBR plasma system test platform are shown in Fig. 1(a) and (b). The whole system consists of three parts: gas distribution system, discharge system and detection system.

The gas distribution system which was used to provide different mixing ratio gases required for the degradation process included a gas distribution meter (GC500, Tunkon Electric Technology Co., Ltd.) and a gas source (Newradar Gas Co., Ltd., Wuhan). The gas distribution meter's maximum output flow rate was 3000 mL $min^{-1}$, gas distribution accuracy ±1% F.S., maximum dilution ratio 300 : 1. The flow rate was controlled by a gas rotameter (50–250 mL $min^{-1}$). The gas used in this test was 99.999% $SF_6$, 99.999% $O_2$ and 99.999% Ar.

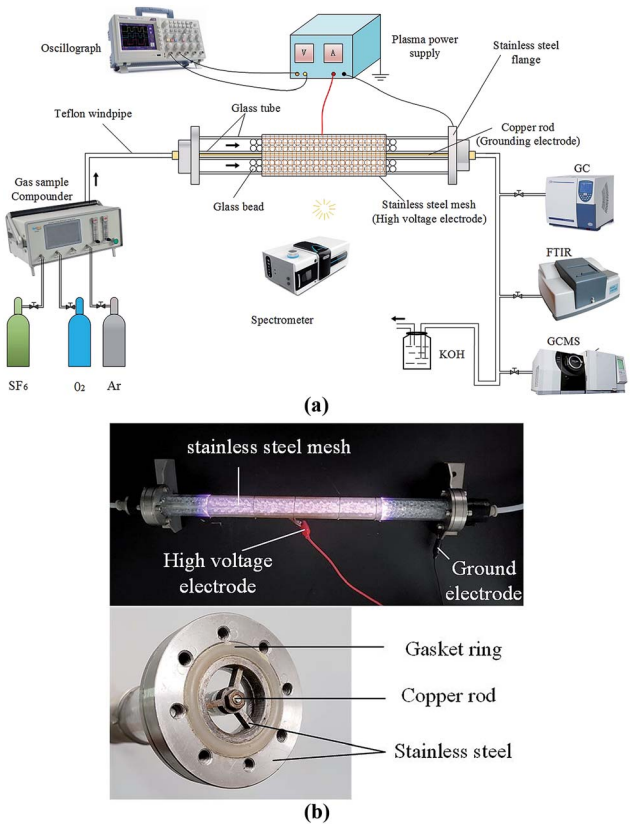


Fig. 1 (a) The schematic diagram of the PBR plasma system test platform. (b) The figure of the PBR.

The discharge system was used to remove $SF_6$, which consisted of a plasma power supply (CTP-2000 K, Nanjing Suman Electronics Co., Ltd.) and a PBR. The plasma was generated by the plasma power supply with discharge working voltage 0–30 kV, output power 0–300 W, discharge frequency 0–20 kHz; a stainless steel mesh (high-voltage electrode) was wrapped tightly around a coaxial dual dielectric quartz tube with dielectric thickness of 2 mm and an inner diameter of 20 mm. The inner ground electrode was a copper rod with an external diameter of 4 mm, installed along the axis of the quartz tube. The discharge length was about 200 mm with a discharge gap of 6 mm. The gap was filled with 3.5 mm diameter glass beads as packing materials. The packing fraction was about 0.59 and the gas gap volume of discharge area was 21.68 $cm^3$. Fixed packing fraction was maintained throughout the test, because this parameter would affect the performance of the whole system.[21]

The detection system consists of a digital oscilloscope (DPO7254C, Tektronix Technology Co., Ltd.), an emission spectrometer (MX2500C, Ocean Optics Co., Ltd.), Gas Chromatograph (GC, GC-450, Shanghai Huishi Instrument), Fourier Transform Infrared Spectrophotometer (FTIR IRTracer-100, SHIMADZU Co., Ltd.) and Gas Chromatography Mass Spectrometer (GC-MS Shimadzu Ultra 2010 plus with CP-Sil 5 CB column, SHIMADZU Co., Ltd.). The digital oscilloscope (4-channel 1G bandwidth, maximum real-time sampling rate 20 GS per s) was used to monitor the instantaneous discharge voltage and current in the PBR. The input power of the plasma power source was read directly from the power supply. The emission spectrometer was a three-channel one which includes three gratings (GRATING_#H5U-UV-UPGD 1200 Line Holographic, H1–H14 and HC-1). It could measure the wavelength from 300 nm to 810 nm, and its optical resolution is 0.1 nm, the integration time was 1 ms to 65 s, and the trigger delay and trigger jitter were 450 ns and 10 ns. The GC was used to detect the concentration of $SF_6$ in the exhaust gas (detector sensitivity was greater than 5000 mV mL $mg^{-1}$, using the area internal standard method). Among them, in the test, GC used 99.999% He as carrier gas, and the peak time of separation $SF_6$ was 2.2–2.4 min. The exhaust gas also passed through GC-MS (inlet temperature was 200 °C, injection was performed in split injection mode with a split ratio of 109 : 1 and inlet pressure of 56.1 kPa); column flow rate was 1.2 mL $min^{-1}$), 99.999% He was used as carrier gas, and internal peak integration method could be used to quantitatively detect $SO_2F_2$, $SOF_2$, $SO_2$, $SOF_4$ four kinds of decomposition gases. The remaining products were qualitatively detected by FTIR. The relevant parameters were: detection band 4000–400 $cm^{-1}$; fraction 1 nm; scan times 10 times; infrared detection pool optical path 10 cm. The tail gas was further treated by a KOH solution scrubber.

The test conditions are summarized as follows: the input power was fixed at 110 W, the power frequency was fixed at 8.7 kHz, Ar was used as the carrier gas to reduce the breakdown voltage of the gas mixture. All the experiments in this paper were conducted at room temperature (298 K) under atmosphere (101.3 kPa). The applied oxygen concentration was 0–8%, and the $SF_6$ concentration was 2–10%. All tests were carried out twice to ensure that the test results were accurate enough.

### 2.2. Parameter calculation method

In this paper, the DRE of $SF_6$ is defined as follows:

$$\mathrm{DRE}(\%) = \frac{C_{\mathrm{in}} - C_{\mathrm{out}}}{C_{\mathrm{in}}} \times 100\% \quad (1)$$

where $C_{\mathrm{in}}$ and $C_{\mathrm{out}}$ refers to the concentrations (ppm, part per million) before and after the treatment.

EY is obtained based on DRE and input power, and the formula is as follows:

$$\mathrm{EY}\left(\mathrm{g\ kW^{-1}\ h^{-1}}\right) = \frac{m_{\mathrm{SF_6}}}{P_{\mathrm{in}}} \quad (2)$$

where $m_{\mathrm{SF_6}}$ is the mass (g) of $SF_6$ degraded per unit time (h) and $P_{\mathrm{in}}$ is the input power (kW) of the plasma power source.

The selectivity equation for the main sulfur-containing products is as follows:

$$S_{\mathrm{K}} = \frac{C_{\mathrm{K}}}{C_{\mathrm{in}} - C_{\mathrm{out}}} \times 100\% \quad (3)$$

Among them, $S_{\mathrm{K}}$ is the concentration of a certain degradation product, $C_{\mathrm{in}}$ and $C_{\mathrm{out}}$ are the concentrations of $SF_6$ before and after the treatment.

## 3 Results and discussion

### 3.1. DRE

Shown in Fig. 2 are DREs plotted against $SF_6$ concentration in the presence of no oxygen, 2% $O_2$ and 8% $O_2$. Noted that the 2% $O_2$ group has the highest DRE, followed by the no $O_2$ group and the lowest in the 8% $O_2$ group. When the concentration of $SF_6$ was 2%, high DREs were obtained under three oxygen concentration conditions. With the increase of $SF_6$ concentration, all DREs decreased, but the no $O_2$ group and the 8% $O_2$ group decreased rapidly while the 2% $O_2$ group decreased slowly.

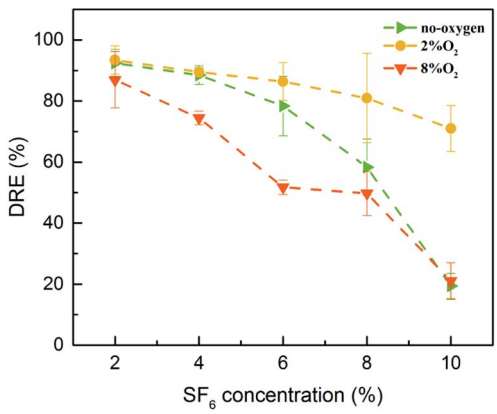


Fig. 2 $SF_6$ DREs under different gas compositions (110 W, 150 mL $min^{-1}$).

Based on the above test results, combined with the study of Zhang *et al.*, this paper summarizes the decomposition process of $SF_6$ into two stages.[22–24] The first stage is the collision decomposition stage of $SF_6$ molecules, which includes the formation of micro-discharge channels, the transport of charges, and the excitation, decomposition, and ionization processes of atoms and molecules.

$$\mathrm{e + Ar \rightarrow e + Ar^*} \quad (4)$$

$$\mathrm{Ar^* + SF_6 \rightarrow SF_{\mathit{x}} + (6 - \mathit{x})F + Ar} \quad (5)$$

$$\mathrm{SF_6 + e \rightarrow SF_{\mathit{x}} + (6 - \mathit{x})F + Ar} \quad (6)$$

where $x = 1, 2, 3, 4, 5$. Ar* refers to the excited state of the argon atom. According to the eqn (4)–(6), there are two ways to decompose $SF_6$. One is caused by the collision of high-energy electrons with $SF_6$ molecules, and the other is caused by the collision of metastable argon atoms with them. When two or more particles undergo an inelastic collision, the S–F bonds in the $SF_6$ molecule are broken to form a low fluorine sulfide and free F radicals. These processes constitute a preliminary decomposition of the $SF_6$ molecules.

Additionally, Fig. 2 shows that when the concentration of $SF_6$ was 2%, the DREs of the no $O_2$ group and the 2% $O_2$ group were 92.50% and 93.42%, respectively; the DRE of 8% $O_2$ group was slightly lower, 86.93%. These results illustrate that when the concentration of $SF_6$ is low, the auxiliary effect of oxygen is not obvious. As the concentration of $SF_6$ increased, the three curves gradually decreased. When the concentration of $SF_6$ reached 10%, the DREs of no $O_2$ group and 8% $O_2$ group decreased significantly, which was 19.43% and 21.03%, respectively. The DRE of 2% $O_2$ group was much higher than that of the previous two groups, which was 71.00%. This is because $SF_6$ is a strong electronegative gas, and a high concentration of $SF_6$ gas absorbs a large amount of seed electrons (electrons before collision) thereby destroying the removal conditions, resulting in lower DREs.

$$\mathrm{SF_{\mathit{x}} + (6 - \mathit{x})F \rightarrow SF_6} \quad (7)$$

The second stage was the recombination of low-fluorine sulfide and the reaction with O radicals. Low-fluorine sulfides were less stable than $SF_6$, and they could easily combine with F radicals to form $SF_6$,[25,26] as shown in eqn (7). When the concentration of $SF_6$ was low, the recombination was not easy to occur because the concentration of $SF_6$ by-products in the reaction zone was also low, and the degradation process of $SF_6$ was much faster than the recombination process. However, as the concentration of $SF_6$ increased, the composite reaction of its products continued to increase. At this point, the recombination must be blocked to achieve better abatement. The addition of $O_2$ blocked the reaction (7), consuming a portion of the low

fluoride, such as eqn (19)–(22) and (27), thereby promoting the $SF_6$ decomposition.

Furthermore, Fig. 2 suggests that when the concentration of $SF_6$ was 6–10%, the DRE of 2% $O_2$ group was much higher than that of no $O_2$ group, because the addition of 2% $O_2$ consumed some low-fluorine sulfide. The recombination of $SF_6$ molecules was slowed down, and more $SF_6$ molecules were decomposed, thus obtaining a higher DRE.

Fig. 3 compared the electrical signals of the no $O_2$ group and the 8% $O_2$ group. The above two figures showed that the phase of the current was ahead of the voltage. This was easy to understand, because the discharge tube was equivalent to a coaxial capacitor, when the air gap was broken down, it could be equivalent to a parallel connection of capacitor and resistance. Moreover, the breakdown of air gap would lead to the distortion of current waveform, because this process made the electrical parameters non-linear. Furthermore, there was no obvious difference between the applied voltage amplitude, but the amplitude and shape of the current waveform were different. Firstly, the current amplitude of 8% oxygen group was slightly smaller than that of no-oxygen group. This might be due to the inhibition of oxygen on discharge, which reduced the charge transfer between electrodes in each discharge cycle. Moreover, it could be seen that the discharge pulse of the no $O_2$ group was more than that of the 8% $O_2$ group, and its amplitude was higher. Therefore, under the same conditions, $O_2$ could weaken the micro-discharge in the reaction tube (the difference in discharge pulse was not obvious when the oxygen concentration was low, so it was not given in this paper). Similar to $SF_6$, this might be because oxygen was also an electronegative gas, which had a good affinity for electrons, and adsorbed a part of free electrons to form negative oxygen ions,[27] resulting in a decrease in free electron density in the reaction region. Accordingly, the charge density of the electrode surface was reduced, and the induced voltage generated by the electrode was also reduced, thereby causing the voltage of the gas to rise and the breakdown voltage thereof to rise accordingly. These changes were detrimental to impact ionization within the reaction tube and result in fewer S–F bonds being broken. This also explained the fact that the DRE of the 8% $O_2$ group in Fig. 2 was always the lowest.

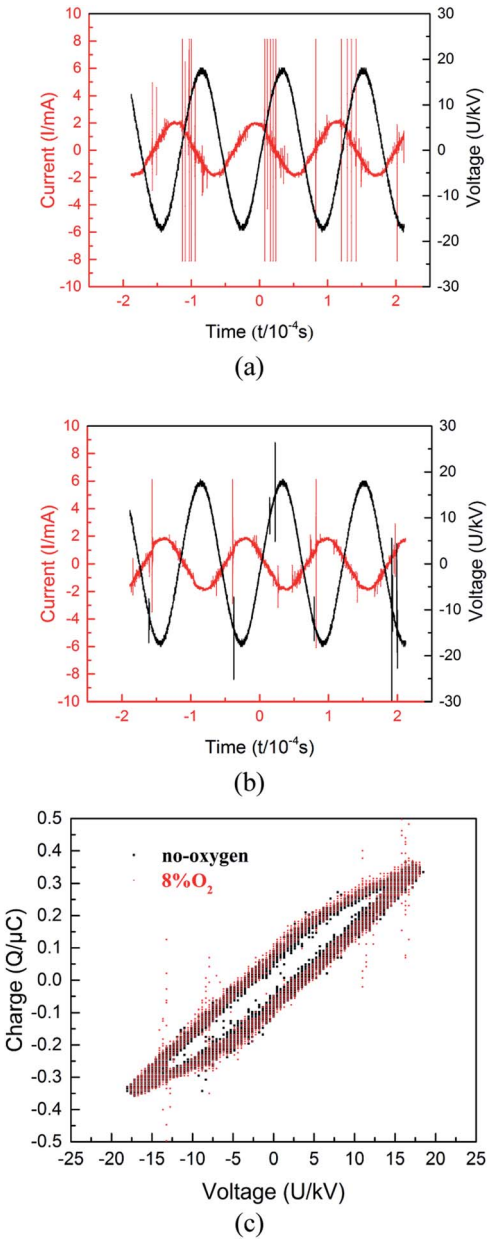


Fig. 3 Electrical signals of the PBR. (a) Voltage and current waveform of no $O_2$ group. (b) Voltage and current waveform of 8% $O_2$ group. (c) Lissajous figures of no-oxygen and 8% $O_2$ (6% $SF_6$, 110 W, 150 mL $min^{-1}$).

Fig. 3(c) shows the Lissajous figures of $SF_6$ abatement at no-oxygen and 8% $O_2$ conditions. The area of the Lissajous figure represents the discharge power in a period and the slope of four edges corresponds to the equivalent capacitance, but as shown in the figure, the addition of oxygen does not change them.[22,28,29] The above phenomena illustrate that the external gas has no effect on the electrical parameters of the discharge circuit. That may be due to the difference of electric constant between oxygen, argon and sulfur hexafluoride can be neglected. Therefore, the addition of oxygen does not change the electrical parameters of PBR.

This section analyzed the effect of oxygen concentration on the DREs of $SF_6$. The discharge current waveform of PBRs proves that excess oxygen will affect its discharge process to hinder the decomposition of $SF_6$. In this context, the oxygen concentration is preferably between 0 and 4%, higher than this value is excessive. However, The DREs decreases with the $SF_6$ concentration in the system, the higher concentration of $SF_6$ was not studied in this paper, because too low DRE makes no sense to reduce emissions.

### 3.2. EY

In Fig. 4, the effect of oxygen concentration on EYs of the PBR degradation under different $SF_6$ concentrations is shown. In this paper, EYs were calculated by DREs. In order to facilitate the observation of the effect of oxygen concentration on EY,

 

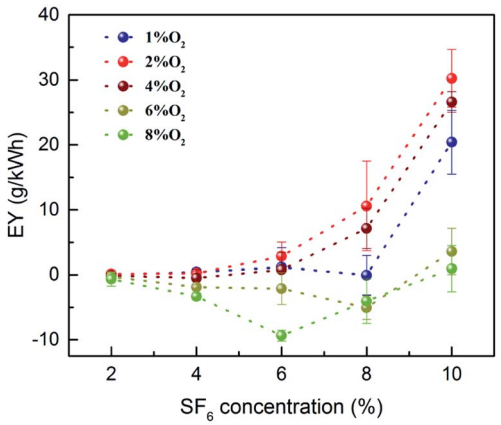


Fig. 4 Effect of different oxygen concentrations on degradation of different concentrations of $SF_6$ (110 W, 150 mL $min^{-1}$, the values in the figure are all after deducting the EY of corresponding no-oxygen condition).

the EY of the oxygen-containing group was subtracted one by one from the EY of the no $O_2$ group. Fig. 4 demonstrates that the EY of 6% $O_2$ and 8% $O_2$ groups are all below the zero line, indicating that oxygen in this concentration range has a negative impact on the $SF_6$ degradation. Meanwhile, the line diagrams of 1%, 2%, and 4% $O_2$ groups are all located above the zero line. It can be seen that $O_2$ promotes the decomposition of $SF_6$ in this oxygen concentration range. Moreover, when the concentration of $SF_6$ was 6% or less, the promoting effect was not obvious, and the promoting effect was obvious when it was higher than 6%.

In this experiment, the highest EY of the no $O_2$ group occurred when the concentration of $SF_6$ was 6%, which was 25.16 g $kW^{-1}$ $h^{-1}$; the highest EY of the oxygen-containing group appeared under the condition of 10% $SF_6$ and 2% $O_2$, which was 37.99 g $kW^{-1}$ $h^{-1}$. The maximum EY increased by 50.99%. This suggests that the addition of 2% $O_2$ enables the PBR to treat higher concentrations of $SF_6$. Fig. 5 compares the literature,[13,14] and the maximum EY obtained in this paper, which shows a significant synergy between the proper amount of oxygen and the PBR.

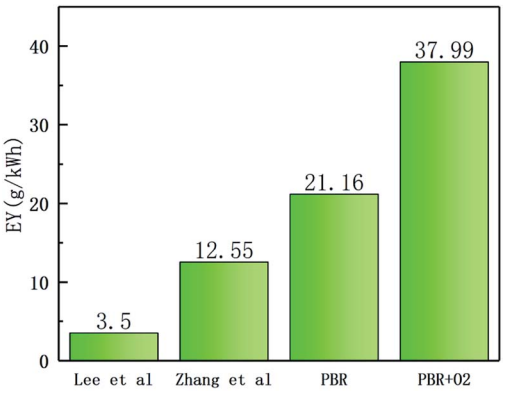


Fig. 5 EYs for different conditions from this study and Lee *et al.*[13] and Zhang *et al.*[14]

The flow rate has a great influence on the degradation of $SF_6$. Under the same experimental conditions, the DRE and EY of $SF_6$ at different flow rates were studied.

The data presented in Fig. 6 shows that as the flow rate increases, the DRE decreased from 93.90% (100 mL $min^{-1}$) to 56.86% (250 mL $min^{-1}$), and the EY increased from 21.81 g $kW^{-1}$ $h^{-1}$ (100 mL $min^{-1}$) to 33.02 g $kW^{-1}$ $h^{-1}$ (250 mL $min^{-1}$). This indicates that $SF_6$ cannot be completely degraded at high flow rates, but the amount of $SF_6$ molecules that were degraded at high flow rates was greater. Within a certain flow rate range (100–250 mL $min^{-1}$, the corresponding average residence time of the mixed gas is 17.34–5.20 s), the number of $SF_6$ molecules entering the PBR per unit time increased with the increase of flow rate, and the average residence time of each $SF_6$ molecule in the PBR was reduced, which causing a part of $SF_6$ to be discharged out of the tube without reaction, thereby reducing the DRE; but at the same time, a larger number of $SF_6$ molecules are degraded, so that the EY increased.

This section analyzed the EY of the PBR at different oxygen concentrations and flow rates, demonstrating a clear synergistic effect between oxygen and the PBR. However, the high EY obtained was accompanied by a lower DRE, which would become an obstacle to improve EY. Such a situation can be solved by secondary degradation, that is, the degraded exhaust gas is again degraded by PBRs.[30,31] Secondly, limited by the size of the device, the PBR used herein is suitable for the abatement of $SF_6$ gas with a flow rate not exceeding 150 mL $min^{-1}$. To handle larger flows of gas, multiple PBRs can be used in parallel, both of which are the subject of our further research.

### 3.3. By-products analysis

**3.3.1. Emission spectrum analysis.** Fig. 7(a) and (b) show the emission spectra of the $SF_6/O_2/Ar$ plasma, and the characteristic lines in them correspond to several reactive species. Compared with the NIST database,[32] the $SF_6/O_2/Ar$ plasma emission was initially diagnosed. Due to the large difference in the proportion of different elements in the $SF_6/O_2/Ar$ system, the intensity difference of the emission spectrum is also large.

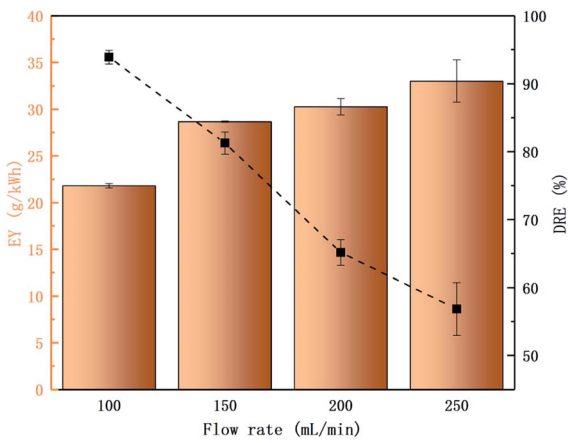


Fig. 6 EY and DRE under different flow rates (6% $SF_6$/2% $O_2$/Ar, 110 W).

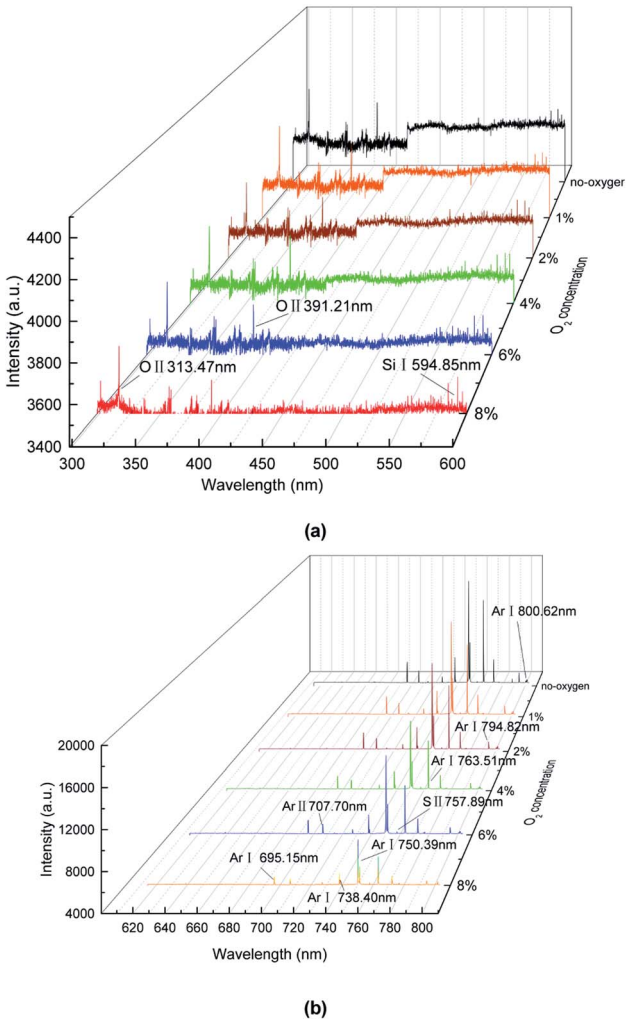


Fig. 7 The emission spectra of the PBR (6% $SF_6$, 110 W). (a) 300–600 nm (b) 600–810 nm.

In order to show the characteristic lines more clearly, the emission spectrum was divided into two sections (300–600 nm (a) and 600–810 nm (b)). Fig. 7(a) shows there is an element detected (Si I 594.85 nm). The intensity of the segment line was low, indicating that the amount of corresponding material was also small. The presence of the Si element indicates that the products of $SF_6$ reacts with the glass wall and the glass tube (etching effect). The purpose of using glass tubes and beads in this paper is to detect the emission spectra better. Meanwhile, glass beads as packing materials can enhance the electric field in the tube.[18]

Fig. 7(b) shows the other two elements detected (Ar I 695.15 nm, Ar I 750.39 nm, nm, Ar I 763.51 nm, Ar I 794.82 nm, Ar I 800.62 nm). Compared with other elements, Ar has the highest line emission intensity because argon has the highest proportion of the whole system, reaching over 86%. These lines show that a large amount of argon atoms were excited. When the energy of electrons exceeds 11.5 eV, argon atoms can be excited. Calculations show that, under this condition, the energy of most of the free electrons in the system can exceed this value, so a large number of argon atoms were excited.[11] Eqn (4) shows the process. In addition, due to the environment noise and the spectrometer error, some spectral lines can not be well diagnosed. We also made a possible analysis of it. Those lines may include O II 313.57 nm, O II 391.51 nm, S II 757.89 and Ar II 707.70 nm. The argon lines have been analyzed previously. In addition, the existence of O radicals may be due to the involvement of oxygen or tube wall ($SiO_2$) in the reaction. Furtherly, the S radicals may be as a result of $SF_6$ molecules decomposition.

Furthermore, Fig. 7(b) shows the intensity of Ar lines decrease with the oxygen concentration. Because the emission line intensity of the spectral line is proportional to the population density of the excited state involved in the optical emission. Under the local thermal equilibrium condition (LTE), the electron temperature was measured by using the well-known Boltzmann plot:[33]

$$kT_e = (E_2 - E_1)\ln\left[\frac{I_1\lambda_1 g_2 A_2}{I_2\lambda_2 g_1 A_1}\right]^{-1} \quad (8)$$

where the indices 1 and 2 are the first and second spectral lines, $k$ is the Boltzmann constant, $I$ is the measured intensity of the spectral lines, $E$ is the energy of the excited states, $g$ is the statistical weight and $A$ is the transition probability. Two Ar-I lines were selected for determination of the electron temperature. These lines were resulted from the $4p^1$ to 4s[0] transition at 794.82 nm and $4p^2$ to $4s^1$ at 800.62 nm and the details are collected in Table 1. The intensities of these Ar-I lines were obtained from the spectrum by integrating over the line profile and normalizing with the spectral response of the sensitivity of the instrument. The electron temperature for different oxygen concentration was obtained by repeating the same procedure.

Fig. 8 shows a decreasing trend in the electron temperature with rise of oxygen concentration. Such descending trend in electron temperature may be due to the decline of electrons kinetic energy in the discharge plasma. For atmospheric pressure PBRs, although the mean free path of the electrons within the discharge remains constant, due to an increase in oxygen concentration, electrons are increasingly affected by the adsorption of oxygen molecules, which eventually leads to less and less energetic electrons are available for plasma chemical reaction. Therefore, the oxygen molecules suppress the excitation and ionizing of the neutral plasma species and consequently the electron temperature.

**3.3.2. FTIR analysis.** In Fig. 9, $SF_6$ degradation by-products were detected by FTIR. The peak information is mainly referred to the research by Kurte and Zhang *et al.*[19,34] In the $SF_6/O_2/Ar$ system, the decomposition products of $SF_6$ are $SO_2F_2$, $SiF_4$, $SOF_2$, $SOF_4$, $SF_4$, $SO_2$, and $OF_2$. This is similar to the conclusion

Table 1 The data of spectral lines

| Lines | $\lambda$ (nm) | $A$ | $E$ ($cm^{-1}$) | $g$ | Ref. |
|---|---|---|---|---|---|
| Ar-I | 794.82 | $1.86 \times 10^7$ | 107 131.71 | 3 | [NIST][32] |
| Ar-I | 800.62 | $4.90 \times 10^6$ | 106 237.55 | 5 | [NIST][32] |

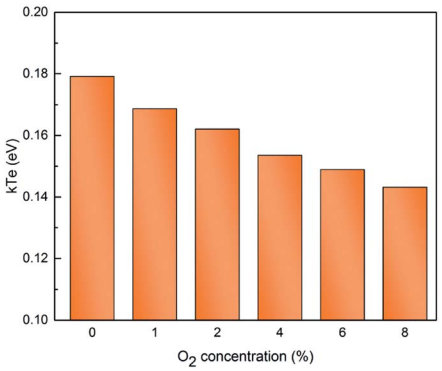


Fig. 8 The electron temperature as a function of oxygen concentration.

of Lee *et al.* Among them, $SO_2F_2$ and $SiF_4$ are the main products, which may be because the two materials are relatively stable, and the presence of $SiF_4$ once again proves the existence of etching effect. By ref. 19, it can be noted that in addition to the above by-products, there should be $S_2F_{10}$, but it is not recognized in the FTIR diagram, probably because the substance is easily decomposed as shown in eqn (28), or it overlaps with the peaks of $SO_2F_2$, which leads to the failure of diagnosis.

**3.3.3. GCMS analysis.** Fig. 10 shows the content of sulfur-containing degradation products measured by GCMS (products include but are not limited to the four substances and the relevant formulas are provided in the Appendix).

Firstly, the concentration of $SO_2F_2$ was the lowest at 12 444.67 parts per million (ppm) under no $O_2$ conditions. As the oxygen concentration reached 4%, the concentration of $SO_2F_2$ reached a maximum of 22 385.36 ppm. This may be because the O radicals in the system were capable of oxidizing $SOF_2$, $SOF_4$ and $SF_X$ to $SO_2F_2$, as shown in eqn (23) and (24). Therefore, as the oxygen concentration boosted, the concentration of $SO_2F_2$ also increased. However, as the oxygen concentration further increased, its concentration began to decrease. When the oxygen concentration was 8%, its concentration was only 17 873.33 ppm. This might be because as the oxygen became excessive, the EY of the system decreased. As shown in Fig. 4, the amount of handled $SF_6$ molecules was correspondingly reduced, eventually resulting in a decrease in products concentration, which contributed to the decrease of $SO_2F_2$.

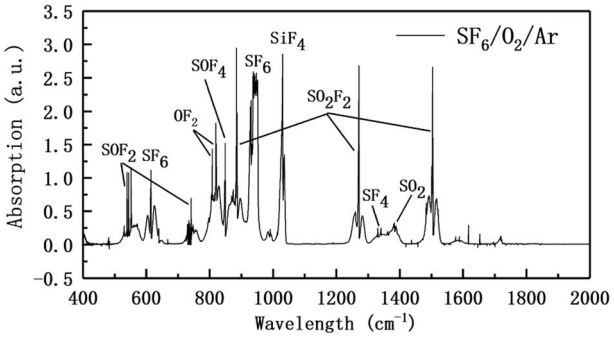


Fig. 9 FTIR spectrum of by-products (6% $SF_6$/2% $O_2$/Ar).

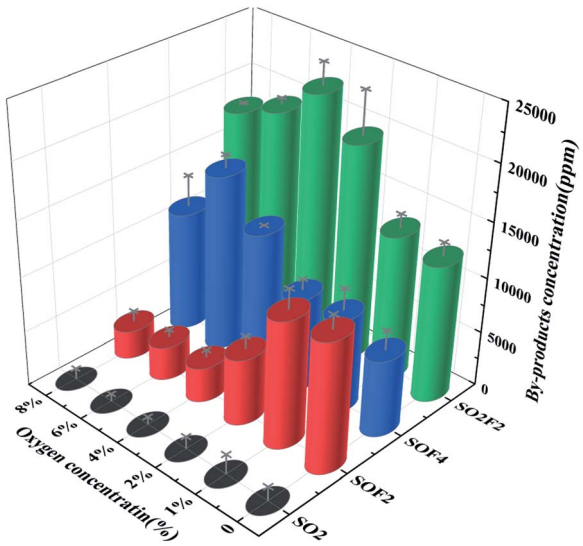


Fig. 10 Four $SF_6$ degradation products concentration (6% $SF_6$/Ar).

Under the no $O_2$ environment, the concentration of $SOF_2$ was the highest, which was 11 820.21 ppm. With the increase of oxygen concentration, the concentration continued to decrease. When the oxygen concentration reached 8%, the concentration of $SOF_2$ was only 2538.07 ppm. This indicated that oxygen has an inhibitory effect on the formation of $SOF_2$. It was known from the

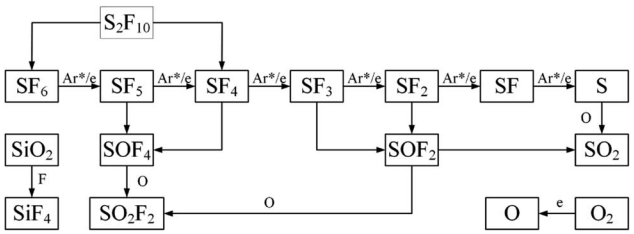


Fig. 11 $SF_6$ degradation path.

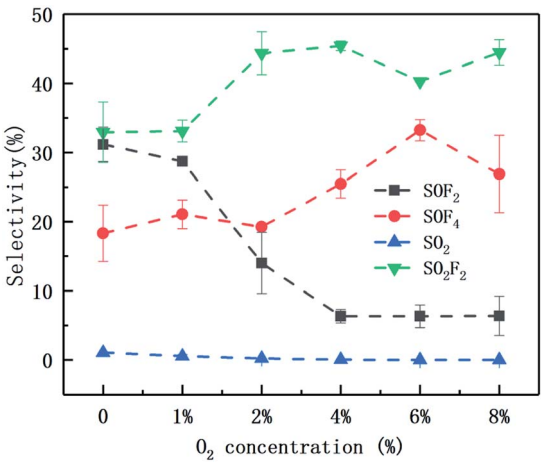


Fig. 12 Selectivity of four products under different oxygen concentrations (6% $SF_6$, 110 W, 150 mL $min^{-1}$).

Table 2 Physicochemical properties of several major degradation products[14]

| Product | Melting point (°C) | Boiling point (°C) | Chemical properties |
|---|---|---|---|
| $SO_2F_2$ | −124.7 | −55.4 | Slow hydrolysis in lye |
| $SOF_2$ | −130 | −43.8 | Hydrolysis produces HF (reacts with lye) and $SO_2$ |
| $SO_2$ | −72.7 | −10 | Reaction with lye |
| $SF_4$ | −99.6 | −49.0 | Hydrolysis produces $SOF_4$ |
| $SOF_4$ | −120 | −55.4 | Hydrolysis produces $SO_2F_2$ and HF |
| $S_2F_{10}$ | −55 | 29 | Easily decomposed into $SF_6$ and $SF_4$ |
| $SiF_4$ | −90 | −86 | Easy to react with alkali to form silicate |

eqn (21), (22) and (24), Table 3 that $SOF_2$ was mainly formed by reacting a low fluorine sulfide with an O radical, and it could further react with an O radical to form $SO_2F_2$. Probably because the secondary oxidation process was faster than the primary oxidation. Therefore, under no $O_2$ condition, the concentration of O radicals in the system was lower, and more $SOF_2$ was generated; as the oxygen concentration increased, more and more $SOF_2$ was further oxidized to form $SO_2F_2$, and meanwhile, the concentration of $SOF_2$ would decrease further as the EY decreased.

The concentration of $SOF_4$ slowly increased with increasing oxygen concentration, reaching a maximum value of 15 975.24 ppm at an oxygen concentration of 6%, and then decreased. From eqn (19)–(20), both $SF_4$ and $SF_5$ could generate $SOF_4$ with O radicals. Meanwhile, it was known from the eqn (23) that the substance can be further oxidized to form $SO_2F_2$. Therefore, as the oxygen concentration increased, more and more low-fluorine sulfides were oxidized to form $SOF_4$, but at the same time, some $SOF_4$ was further oxidized. Consequently, overall showing a slow increase in $SOF_4$ concentration. When the oxygen concentration was excessive, the low EY of the system also leaded to a decrease in the concentration of $SOF_4$.

The concentration of $SO_2$ decreased with the increase of oxygen concentration, refer to the reaction eqn (25) and (26). It could be observed that the reaction to generate $SO_2$ was not much, and eqn (25) was the easiest to occur, but at the same time, it was known from eqn (13)–(18) that S radicals are extremely low in the system because only the six S–F bonds of $SF_6$ broken could it generate a S radical. Eqn (26) should be the main generation path of $SO_2$, but as the reactant $SOF_2$ decreased sharply, the $SO_2$ generated by the path also decreases rapidly. The degradation path of $SF_6$ was in Fig. 11.

Fig. 12 shows the selectivity of four products as a function of oxygen concentration during 6% $SF_6$ gas degradation. The selectivity of $SO_2F_2$ is always the highest, ranging from 32.93% to 45.43%, because the substance has the highest stability and is the final product of $SF_6$ (as shown in the Fig. 11). The selectivity of $SO_2$ is always low, close to zero, and has been analyzed from its source. The selectivity of $SOF_2$ and $SOF_4$ changed greatly with the increase of oxygen concentration. When the oxygen concentration is less than 2%, the selectivity of $SOF_2$ is greater than $SOF_4$, otherwise, $SOF_4$ is more selective. This may be because when the oxygen concentration is low, the source of O radicals in the system is mainly $SiO_2$. As shown in eqn (29), $SiO_2$ can react with four F radicals to form $SiF_4$ and two O radicals. As the oxygen concentration increases, the concentration of O radicals in the system increases, which undoubtedly inhibits the participation of $SiO_2$, causing the content of $SiF_4$ in the product is relatively reduced, while one $SOF_4$ molecule is capable of immobilizing 4 F atoms. Therefore, $SOF_4$ is more selective at higher oxygen concentrations.

Table 2 lists the physicochemical properties of several major products. $SO_2F_2$, $SOF_2$, $SO_2$, $SF_4$, $SOF_4$ can react with lye (KOH) to form KF and $K_2SO_4$, which effectively prevents the products from recombination and can also achieve the further processing of products.[35]

In this part, the reactive species, electron temperature and products in the degradation process of $SF_6$ were analyzed by emission spectrometer, FTIR and GCMS, and the decomposition path of $SF_6$ in oxygen-containing environment was summarized. The concentration variation and selectivity of four products at different oxygen concentrations were discussed, demonstrating that oxygen participates in the second stage of the $SF_6$ degradation process, that was, the process of combining low-fluoride sulfide with reactive species such as O to form secondary degradation products to affect the decomposition of $SF_6$. The by-products also confirmed that the concentration of the applied gas can also affect the selectivity of the products.

## 4. Conclusion

In this paper, the degradation of high concentration $SF_6$ by the PBR was carried out at different oxygen concentrations. The synergistic effect of oxygen and the PBR on $SF_6$ degradation was investigated.

The results show that an appropriate amount of oxygen in the system can greatly improve the EY of $SF_6$ degradation in the PBR. The highest EY can be obtained when the concentration of $SF_6$ is 10%, which is 37.99 g $kW^{-1}$ $h^{-1}$ under the condition of 2% $O_2$. However, when the oxygen in the system is excessive, the degradation effect will be worse than that of the no $O_2$ group. Moreover, the current waveform of PBR also demonstrates that 8% $O_2$ has a weakening effect on the microdischarge. From the perspective of EY, oxygen concentration within 4% promotes degradation, above which it hinders

 

degradation. Meanwhile, the flow rate can significantly affect the degradation efficiency. In the flow rate range of this paper, the DRE decreases with the increase of the flow rate, and the EY increases with the increase of the flow rate. Furthermore, the exist of active radicals such as Ar and Si suggests the exciting process in the PBR. The intensity of the emission spectra and electron temperature reveal the fact that the addition of oxygen will suppress the collision in the system and weaken the degradation effect. In addition, the products obtained herein mainly include $SO_2F_2$, $SiF_4$, $SOF_2$, $SOF_4$, $SF_4$, $SO_2$ and so on. Among the four degradation products ($SO_2F_2$, $SOF_2$, $SOF_4$, $SO_2$) of $SF_6$ under all conditions, the highest selectivity is $SO_2F_2$, and the lowest selectivity is $SO_2$. The concentration and selectivity of $SOF_2$ and $SOF_4$ are related to the oxygen concentration. When the oxygen concentration does not exceed 2%, the $SOF_2$ selectivity is higher than $SOF_4$ in the degradation process of 6% $SF_6$. Conversely, $SOF_4$ selectivity is higher than $SOF_2$.

It is proved that the EY can be improved and the product selection could be adjusted by controlling the oxygen concentration in the PBR plasma system. This paper provided experimental support for further engineering application of $SF_6$ exhaust gas treatment and better understanding of the effect of oxygen concentration has on the $SF_6$ degradation in a PBR.

## Appendix

Table 3 Reaction formula and reaction heat of $SF_6$ degradation process

| No | Reaction | Reaction heat (kcal $mol^{-1}$) |
|---|---|---|
| (9) | $e^* + O_2 \rightarrow O + O + e$ | 112.51 |
| (10) | $e^* + O_2 \rightarrow O + O^-$ | 90.57 |
| (11) | $e^* + O_2 \rightarrow O^+ + O + 2e$ | 324.53 |
| (12) | $O^- \rightarrow O + e$ | 21.05 |
| (13) | $SF_6 \rightarrow F + SF_5$ | 86.09 |
| (14) | $SF_5 \rightarrow F + SF_4$ | 41.46 |
| (15) | $SF_4 \rightarrow F + SF_3$ | 97.15 |
| (16) | $SF_3 \rightarrow F + SF_2$ | 53.32 |
| (17) | $SF_2 \rightarrow F + SF$ | 86.18 |
| (18) | $SF \rightarrow F + S$ | 113.79 |
| (19) | $SF_5 + O \rightarrow SOF_4 + F$ | −42.53 |
| (20) | $SF_4 + O \rightarrow SOF_4$ | −126.63 |
| (21) | $SF_3 + O \rightarrow SOF_2 + F$ | −77.57 |
| (22) | $SF_2 + O \rightarrow SOF_2$ | −130.89 |
| (23) | $SOF_4 + O \rightarrow SO_2F_2 + 2F$ | −87.39 |
| (24) | $SOF_2 + O \rightarrow SO_2F_2$ | −39.03 |
| (25) | $S + 2O \rightarrow SO_2$ | −274.71 |
| (26) | $SOF_2 + O \rightarrow SO_2 + 2F$ | −68.33 |
| (27) | $2F + O \rightarrow OF_2$ | — |
| (28) | $S_2F_{10} \rightarrow SF_4 + SF_6$ | — |
| (29) | $SiO_2 + 4F \rightarrow SiF_4 + 2O$ | — |

## Conflicts of interest

There are no conflicts to declare.

## Acknowledgements

This work was supported by the National Natural Science Foundation of China (NSFC, under Grant 51777144) and State Grid Science and Technology Project (SGHB0000KXJS1800554).

## References

1 J. Reilly, *et al.*, Multi-gas assessment of the Kyoto protocol, *Nature*, 1999, **401**(6753), 549–555.
2 Y. Li, X. Zhang, S. Tian, S. Xiao, Y. Li and D. Chen, Insight into the decomposition mechanism of $C_6F_{12}O$–$CO_2$ gas mixture, *Chem. Eng. J.*, 2019, **360**, 929–940.
3 Y. Li, X. Zhang, J. Zhang, S. Xiao, B. Xie, D. Chen, Y. Gao and J. Tang, Assessment on the toxicity and application risk of $C_4F_7N$: a new $SF_6$ alternative gas, *J. Hazard. Mater.*, 2019, **368**, 653–660.
4 Y. Li, X. Zhang, J. Zhang, X. Cheng, X. Shao, Z. Wang, D. Chen and X. Song, Study on the thermal decomposition characteristics of $C_4F_7N$–$CO_2$ mixture as eco-friendly gas insulating medium, *High Voltage*, DOI: 10.1049/high voltage.2019.0032.
5 M. Rabie and C. M. Franck, Assessment of eco-friendly gases for elec-trical insulation to replace the most potent industrial greenhouse gas $SF_6$, *Environ. Sci. Technol.*, 2018, **52**(2), 369-380.
6 M. Shih, W.-J. Lee and C.-Y. Chen, Decomposition of $SF_6$ and $H_2S$ Mixture in Radio Frequency Plasma Environment, *Ind. Eng. Chem. Res.*, 2003, **42**, 2906–2912.
7 C.-H. Tsai and J.-M. Shao, Formation of fluorine for abating sulfur hexafluoride in an atmospheric-pressure plasma environment, *J. Hazard. Mater.*, 2008, **157**, 201–206.
8 X. Song, X. Liu, Z. Ye, J. He, R. Zhang and H. Hou, Photodegradation of $SF_6$ on polyisoprene surface: implication on elimination of toxic byproducts, *J. Hazard. Mater.*, 2009, **168**, 493–500.
9 X. Wang, Dielectric Barrier Discharge and Its Application, *High Voltage*, 2009, **35**(1), 1–11.
10 T. Shao, Z. Cheng, W. Ruixue, *et al.*, Atmospheric-pressure pulsed gas discharge and pulsed plasma application, *High Voltage.*, 2016, **42**(3), 685–706.
11 X. Zhang, H. Xiao and X. Hu, Effects of Reduced Electric Field on Sulfur Hexafluoride Removal for a Double Dielectric Barrier Discharge Reactor, *IEEE Trans. Plasma Sci.*, 2018, **46**(3), 563–570.
12 X. Zhang, H. Xiao, J. Tang, *et al.*, Recent advances in decomposition of the most potent greenhouse gas $SF_6$, *Crit. Rev. Environ. Sci. Technol.*, 2017, **47**(18), 1763–1782.
13 H. M. Lee, M. B. Chang and K. Y. Wu, Abatement of sulfur hexafluoride emissions from the semiconductor manufacturing process by atmospheric pressure plasmas, *J. Air Waste Manage. Assoc.*, 2004, **54**(8), 960–970.

14 X. Zhang, Z. Cui, Y. Li, *et al.*, Abatement of $SF_6$ in the presence of $NH_3$ by dielectric barrier discharge plasma, *J. Hazard. Mater.*, 2018, **360**, 341–348.

15 H. L. Chen, H. M. Lee, S. H. Chen and M. B. Chang, Review of Packed-Bed Plasma Reactor for Ozone Generation .and Air Pollution Control, *Ind. Eng. Chem. Res.*, 2008, **47**, 2122–2130.

16 C. L. Chang and T. S. Lin, Decomposition of Toluene and Acetone in Packed Dielectric Barrier Discharge Reactors, *Plasma Chem. Plasma Process.*, 2005, **25**(3), 227–243.

17 H. H. Kim, H. Kobara, A. Ogata and S. Futamura, Comparative Assessment of Different Non-thermal Plasma Reactors on Energy Efficiency and Aerosol Formation from the Decomposition of Gas-Phase Benzene, *IEEE Trans. Ind. Appl.*, 2005, **41**(1), 206–214.

18 H. L. Chen, H.-M. Lee, L. Cheng, M. B. Chang, S. J. Yu and S. Li, Influence of Nonthermal Plasma Reactor Type on $CF_4$ and $SF_6$ Abatements, *IEEE Trans. Plasma Sci.*, 2008, **36**(2), 509–516.

19 X. Zhang, Z. Cui, Y. LI, H. Xiao, L. Yi and J. Tang, Study on Degradation of $SF_6$ in the Presence of $H_2O$ and $O_2$ Using Dielectric Barrier Discharge, *IEEE Access*, 2018, **6**, 72748–72756.

20 Y. S. Mok and D.-H. Kim, Decomposition of Sulfur Hexafluoride by Using a Nonthermal Plasma-assisted Catalytic Process, *J. Korean Phys. Soc.*, 2011, **59**(61), 34–37.

21 M. Y. Naz and S. A. Sulaiman, PTV profiling of particles motion from the top and side of a swirling fluidized bed, *J. Instrum.*, 2016, **11**(5), P05019–P05036.

22 X. Zhang, X. Hu, Z. Cui, *et al.*, Experimental study on the effect of different background gases on the degradation of $SF_6$ gas by dielectric barrier discharge, *J. Electrical. Eng. Technol.*, 2018, **38**(3), 937–946.

23 H. Xiao, X. Zhang, X. Hu, *et al.*, Experimental and simulation analysis on by-products of treatment of $SF_6$ using dielectric barrier discharge, *IEEE Trans. Dielectr. Electr. Insul.*, 2017, **24**(3), 1617–1624.

24 X. Zhang, W. Yao, J. Tang, *et al.*, Current Status and Development of Gas Fraction Analysis of $SF_6$ Discharge Decomposition, *High Voltage*, 2008, **34**(4), 664–747.

25 J. Tang, F. Liu, Q. Meng, *et al.*, Partial Discharge Recognition through an Analysis of $SF_6$ Decomposition Products Part 2: Feature Extraction and Decision Tree-based Pattern Recognition, *IEEE Trans. Dielectr. Electr. Insul.*, 2012, **19**(1), 37–44.

26 D. Chen, X. Zhang, H. Xiong, Y. Li, J. Tang, S. Xiao and D. Zhang, A first-principles study of the $SF_6$ decomposed products adsorbed over defective $WS_2$ monolayer as promising gas sensing device, *IEEE Trans. Device Mater. Reliab.*, 2019, **19**(3), 473–483.

27 H. Xiao, *Study on atmospheric pressure dielectric barrier discharge and its synergistic catalytic degradation of $SF_6$ gas*, Ph.D thesis, Chongqing University, 2018.

28 T. Butterworth, R. Elder and R. Allen, Effects of particle size on $CO_2$ reduction and discharge characteristics in a packed bed plasma reactor, *Chem. Eng. J.*, 2016, **293**, 55–67.

29 D. Mei, X. Zhu, Y.-L. He, D. Y. Joseph and X. Tu, Plasma-assisted conversion of $CO_2$ in a dielectric barrier discharge reactor: understanding the effect of packing materials, *Plasma Sources Sci. Technol.*, 2015, **24**, 015011.

30 H. M. Lee, M. B. Chang and R. F. Lu, Abatement of Perfluorocompounds by Tandem Packed-Bed Plasmas for Semiconductor Manufacturing Processes, *Ind. Eng. Chem. Res.*, 2005, **44**, 5526–5534.

31 K. R. Ryan and I. C. Plumb, Gas-phase combination reactions of $SF_4$ and $SF_5$ with F in plasmas of $SF_6$, *Plasma Chem. Plasma Process.*, 1988, **8**(3), 281–291.

32 *NIST Atomic Spectra Database Lines Data*, [on line], https://physics.nist.gov/cgibin/ASD.

33 M. Y. Naz, S. Shukrullah, A. Ghaffar, N. U. Rehman and M. Sagir, A Low-Frequency Dielectric Barrier Discharge System Design for Textile Treatment, *Synth. React. Inorg., Met.-Org., Nano-Met. Chem.*, 2016, **46**(1), 104–109.

34 R. K. C. Beyer and H. M. H. D. Klockow, Application of infrared spectroscopy to monitoring gas insulated high-voltage equipment: electrode material-dependent $SF_6$ decomposition, *Anal. Bioanal. Chem.*, 2002, **373**, 639–646.

35 J. Wang, Decomposition gas and treatment of sulfur hexafluoride, *Chem. Propellants Polym. Mater.*, 2003, **1**(6), 16–18.

 